Cell Reports

Report

The Binding Interface between Human APOBEC3F and HIV-1 Vif Elucidated by Genetic and Computational Approaches

Graphical Abstract

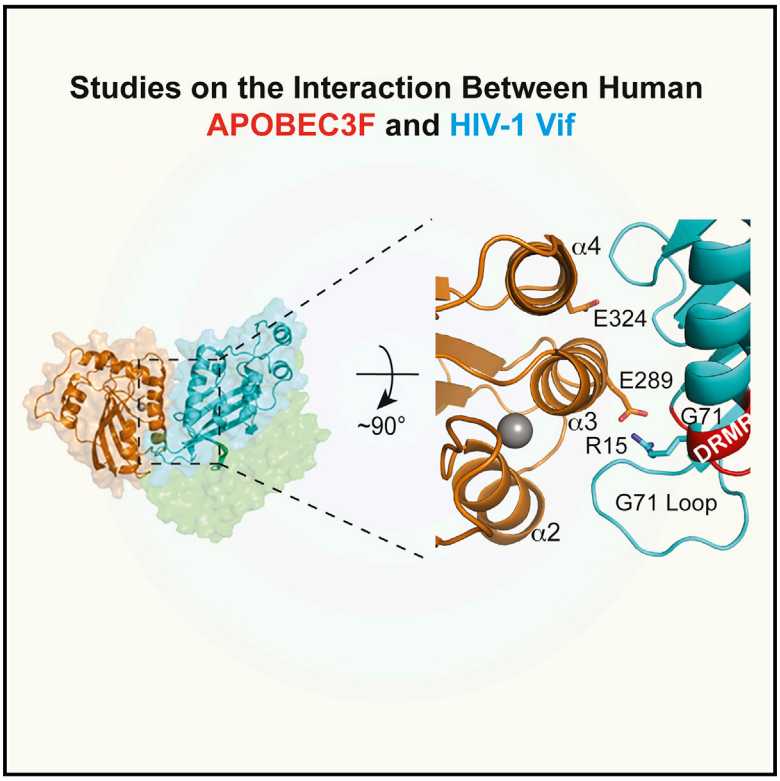

Authors

Christopher Richards, John S. Albin, Özlem Demir, ..., Daniel A. Harki, Rommie E. Amaro, Reuben S. Harris

Correspondence

rsh@umn.edu

In Brief

Richards et al. report a comprehensive structural model to explain how HIV-1 Vif mediates viral pathogenesis by binding to and effecting the degradation of the antiviral enzyme APOBEC3F. Additionally, a wobble model is proposed to explain the rapid evolution of this and other direct pathogen-host interactions.

Highlights

- HIV pathogenesis requires Vif-mediated degradation of host APOBEC3 enzymes
- Virus adaptation and MD simulation experiments reveal interacting amino acids
- These studies inform a structural model of the Vif-APOBEC3F interaction
- A wobble model is proposed to explain the evolution of pathogen-host interactions

Richards et al., 2015, Cell Reports *13*, 1781–1788
December 1, 2015
http://dx.doi.org/10.1016/j.celrep.2015.10.067

CellPress

Cell Reports
Report

The Binding Interface between Human APOBEC3F and HIV-1 Vif Elucidated by Genetic and Computational Approaches

Christopher Richards,[1,2,3,11] John S. Albin,[1,2,3,7,11] Özlem Demir,[4] Nadine M. Shaban,[1,2,3] Elizabeth M. Luengas,[1,2,3] Allison M. Land,[1,2,3,8] Brett D. Anderson,[1,2,3] John R. Holten,[1,2,3,9] John S. Anderson,[1,2,3,10] Daniel A. Harki,[3,5] Rommie E. Amaro,[4] and Reuben S. Harris[1,2,3,6,*]

[1]Department of Biochemistry, Molecular Biology and Biophysics, University of Minnesota, Minneapolis, MN 55455, USA
[2]Institute for Molecular Virology, University of Minnesota, Minneapolis, MN 55455, USA
[3]Masonic Cancer Center, University of Minnesota, Minneapolis, MN 55455, USA
[4]Department of Chemistry and Biochemistry, University of California, San Diego, La Jolla, CA 92093, USA
[5]Department of Medicinal Chemistry, University of Minnesota, Minneapolis, MN 55455, USA
[6]Howard Hughes Medical Institute, University of Minnesota, Minneapolis, MN 55455, USA
[7]Present address: Department of Medicine, Massachusetts General Hospital, Boston, MA 02114, USA
[8]Present address: Department of Biological Sciences, Minnesota State University Mankato, Mankato, MN 56001, USA
[9]Present address: School of Medicine, Temple University, 3500 North Broad Street, Philadelphia, PA 19140, USA
[10]Present address: College of Osteopathic Medicine, Des Moines University, 3200 Grand Avenue, Des Moines, IA 50312, USA
[11]Co-first author
*Correspondence: rsh@umn.edu
http://dx.doi.org/10.1016/j.celrep.2015.10.067

SUMMARY

APOBEC3 family DNA cytosine deaminases provide overlapping defenses against pathogen infections. However, most viruses have elaborate evasion mechanisms such as the HIV-1 Vif protein, which subverts cellular CBF-β and a polyubiquitin ligase complex to neutralize these enzymes. Despite advances in APOBEC3 and Vif biology, a full understanding of this direct host-pathogen conflict has been elusive. We combine virus adaptation and computational studies to interrogate the APOBEC3F-Vif interface and build a robust structural model. A recurring compensatory amino acid substitution from adaptation experiments provided an initial docking constraint, and microsecond molecular dynamic simulations optimized interface contacts. Virus infectivity experiments validated a long-lasting electrostatic interaction between APOBEC3F E289 and HIV-1 Vif R15. Taken together with mutagenesis results, we propose a wobble model to explain how HIV-1 Vif has evolved to bind different APOBEC3 enzymes and, more generally, how pathogens may evolve to escape innate host defenses.

INTRODUCTION

The APOBEC3 (A3) family of DNA cytosine deaminases comprises a powerful arm of the innate immune defense system in mammals. These enzymes provide overlapping protection against highly diverse DNA-based pathogens including transposable elements and viruses (reviewed by Desimmie et al., 2014 and Harris and Dudley, 2015). For instance, four A3 enzymes, APOBEC3D (A3D), APOBEC3F (A3F), APOBEC3G (A3G), and APOBEC3H (A3H), each act to suppress HIV type 1 (HIV-1) replication by packaging into newly synthesized viral particles, directly interfering with reverse transcription, and mutating nascent cDNA cytosines to uracils (reviewed by Desimmie et al., 2014 and Harris and Dudley, 2015). The latter become viral genomic strand guanine-to-adenine (G-to-A) mutations.

To counteract the deleterious effects of these enzymes, HIV-1 encodes a protein called virion infectivity factor (Vif) that scaffolds the formation of an E3 ubiquitin ligase complex that directly binds restrictive A3 enzymes and targets them for proteasome-mediated degradation (reviewed by Desimmie et al., 2014 and Harris and Dudley, 2015). The Vif protein of primate lentiviruses HIV-1, HIV-2, and simian immunodeficiency virus (SIV) has evolved to dimerize with the transcription cofactor CBF-β (Anderson and Harris, 2015 and references therein). This complex enables Vif to additionally bind ELOC and CUL5 and, through these partners, also to ELOB and RBX2. Upon the addition of NEDD8 to CUL5, this E3 ligation assembly becomes activated to transfer ubiquitin from an E2 enzyme to Vif-engaged A3 substrates. Proteomic approaches have been instrumental in identifying Vif ligase components, and genetic studies have demonstrated the essential nature of all of the subunits. A crystal structure of HIV-1 Vif-CBF-β-ELOB-ELOC-CUL5 has helped to rationalize prior results (Guo et al., 2014).

A3F is a notable HIV-1 restriction factor for multiple reasons. First, overexpression causes a dose-responsive drop in the infectivity of Vif-defective viruses and inflicts mutations in a GA-to-AA context (minus strand TC-to-TT) (Bishop et al., 2004; Liddament et al., 2004; Wiegand et al., 2004; Zheng et al., 2004). Second, knockout and knockdown experiments demonstrate

that endogenous levels of this enzyme contribute to HIV-1 restriction and hypermutation in a CD4-positive T cell line and, together with A3D and A3H, account for the GA-to-AA hypermutation signature observed in patient-derived viral sequences (Refsland et al., 2012). Third, HIV-1 restriction activity is conserved between human and rhesus macaque A3F (Hultquist et al., 2011; Virgen and Hatziioannou, 2007; Zennou and Bieniasz, 2006). Fourth, both Vif-binding and DNA cytosine deaminase activities reside within a single zinc-coordinating domain, unlike A3G where these activities are split between the N- and C-terminal domains, respectively (Haché et al., 2005; Russell et al., 2009). Fifth, multiple high-resolution structures and mutagenesis studies have indicated that the Vif-binding surface of A3F is similar to that of A3D and APOBEC3C (A3C), but at least partially distinct from those of A3G and A3H (Albin et al., 2010b; Bohn et al., 2013; Kitamura et al., 2012; Kouno et al., 2015; Land et al., 2014; Russell et al., 2009; Schröfelbauer et al., 2006; Siu et al., 2013; Smith and Pathak, 2010). Sixth, HIV-1 Vif separation-of-function mutants demonstrated the importance of A3F in humanized mouse models for viral pathogenesis (Krisko et al., 2013; Sato et al., 2014). Finally, in long-term cell culture experiments, A3F is sufficiently potent to suppress Vif-deficient HIV-1 replication and select for Vif restoration-of-function mutants (Albin et al., 2010a). This final point is important because it indicates that HIV-1 requires Vif function in order to antagonize A3F and preserve the capacity to replicate. It also implies that HIV-1 cannot easily evolve a Vif-independent mechanism to evade A3F, which further distinguishes this enzyme from multiple Vif-independent mechanisms that the virus may employ to escape A3G restriction (Haché et al., 2008). In other words, the A3F-Vif interaction is essential from an HIV-1 perspective.

Despite these and other advances in the overall understanding of Vif and A3 biology, it is still not clear how Vif actually binds to an A3 substrate. Here, we leverage the selective potential of A3F and virus adaptation studies to identify A3F-interacting amino acid residues within Vif. A recurring genetic contact provided an anchor point for docking the two proteins and deriving a physical interaction model. Molecular dynamic (MD) simulations led to a refined Vif-A3F interaction model that predicted a durable anchoring electrostatic interaction. Charge-reversing substitutions in either A3F (E289K) or Vif (R15E) abrogated the interaction, but the combined amino acid charge changes enabled the interaction to be restored as evidenced by A3F degradation and high viral infectivity. Genetic gain-of-function data were therefore instrumental in both informing the initial model as well as validating the refined model. Our Vif-A3F interaction model also explains prior loss-of-function observations. Overall, our multidisciplinary approach has yielded a comprehensive three-dimensional structural model of this critical pathogen-host interface and also inspired a general wobble model to explain the rapid evolution of this and other pathogen-host interactions.

RESULTS

HIV-1 Adapts to Replicate in the Presence of Vif-Resistant A3F

The lentiviral Vif protein is thought to have evolved to selectively neutralize the A3 repertoire of cognate host species (reviewed by Desimmie et al., 2014 and Harris and Dudley, 2015). Consequently, virus replication is typically restricted by A3s of non-cognate species. For example, the replacement of human A3F (huA3F) residues E324 with the corresponding rhesus macaque A3F (rhA3F) residues K324 renders the human enzyme resistant to degradation by HIV-1 Vif (Albin et al., 2010b; Land et al., 2014; below). We therefore hypothesized that cells expressing this simianized form of huA3F or the naturally restrictive rhA3F (Hultquist et al., 2011; Virgen and Hatziioannou, 2007) would provide selective pressure to force HIV-1 to adapt by making compensatory changes in Vif, analogous to the way that ancestral SIV strains may have adapted in order to transmit into the human population (Figure 1A).

To test this hypothesis, HIV-1_{IIIB} and HIV-$1_{LAI\text{-}GFP}$ stocks were used in graded selection experiments with each passage containing increasing proportions of SupT11 clones stably expressing either huA3F QE323-324EK or rhA3F (i.e., permissive T cells rendered non-permissive through stable expression of these restrictive A3 enzymes). A3F levels in low-expressing T cell lines approximated those in primary CD4-positive T cells (Land et al., 2014), whereas those in medium- and high-expressing lines were intentionally super-physiological (Figure 1B). This approach allows viral sequence diversity to accumulate while selecting for compensatory changes. In total, four rounds of stepwise selection were performed, followed by four additional rounds of MOI-controlled passages under 100% non-permissive conditions to select high-fitness viruses (Experimental Procedures).

Dozens of independent adapted viral populations were obtained as evidenced by similar replication kinetics in permissive SupT11 control cells and non-permissive A3F-expressing derivatives. Adapted variants were identified by sequencing *vif* from proviral DNA, and a clear hotspot emerged with Vif G71D dominating both selective conditions (Figure 1C). Although other amino acid substitutions occurred, none was as prominent as Vif G71D and none apart from Vif G71D yielded a clear phenotype in the context of an otherwise clean molecular clone (G71D data below and additional data not shown; the identities of all amino acid changes occurring in two or more independent cultures are listed in Figure 1C relative to previously implicated interaction motifs in HIV-1 Vif).

HIV-1 Vif G71 Influences the Interaction with A3F

To determine whether HIV-1 Vif G71D overcomes restriction barriers imposed by huA3F QE323-324EK and rhA3F, single-cycle infectivity experiments were done with Vif G71D versus wild-type huA3F, huA3F E324K, and rhA3F. As shown in Figure 2A, G71D mutants displayed modest loss of function in neutralizing wild-type huA3F, but gained significant activity against huA3F E324K and rhA3F. Spreading infection data corroborated these results as Vif G71D engineered into the parental HIV-1_{IIIB} molecular clone, with no other amino acid changes, became attenuated in cells expressing medium and high levels of huA3F, but clearly gained the capacity to replicate in the presence of huA3F E324K (Figure 2B). Peak spreading infection titers did not appear to be affected but a kinetic delay was observed, suggesting that the single G71D change is sufficient to overcome restriction but not optimal for virus replication. Analogous results

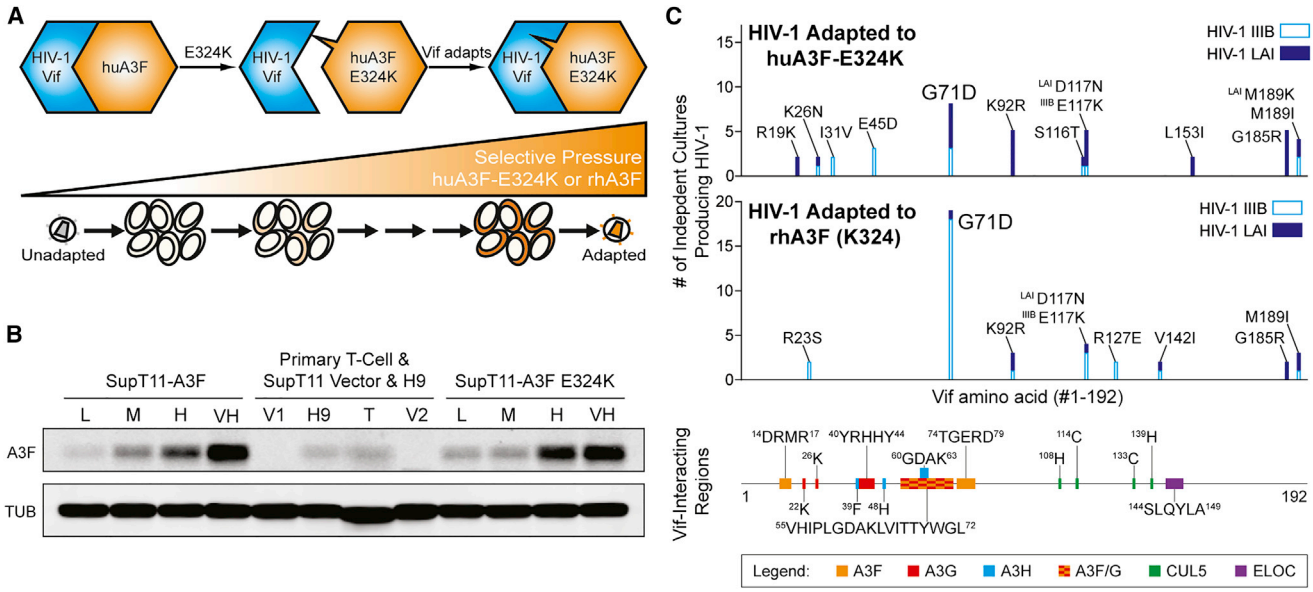

Figure 1. HIV-1 Adaptation to Vif-Resistant A3F

(A) A schematic depicting the co-culture selection strategy used to adapt HIV-1 to Vif-resistant A3F-expressing cells as the selective pressure. Viruses were passaged stepwise approximately every 8–11 days from permissive to increasingly non-permissive cultures as shown. Upon completing a round of selection from fully permissive to fully non-permissive cultures, portions of each culture were cycled back to the beginning of the process for another round of selection. (B) Anti-A3F immunoblot of SupT11-derived T cell lines stably expressing huA3F, A3F QE323-324EK, or empty vector (relative protein expression levels as follows: L, low; M, medium; H, high; VH, very high; and V, empty vector). A3F levels in HIV-1-infected primary T cell and H9 lysates are shown for comparison. (C) Bar graphs indicating the number of independent times that each of the indicated HIV-1 IIIB or LAI Vif amino acid changes were observed. The x axis is a to-scale depiction of Vif residues 1–192 with previously reported motifs indicated below for reference. In most instances, HIV-1_{IIIB} and HIV-1_{LAI} had the same amino acid change at a given position with the exception of HIV-1_{IIIB} E117K and HIV-1_{LAI} D117N for both A3F QE323-324EK and rhA3F selective conditions (shown explicitly in the figure).

were obtained for spreading infection experiments with HIV-1 Vif G71 versus D71 molecular clones in SupT11 cells stably expressing rhA3F (Figure S1).

Delineation of the Vif-A3F Interface

The gain-of-function amino acid substitution G71D selected in adaptation experiments with both huA3F E324K and rhA3F suggested that these two residues are physically interacting. This possibility is consistent with the crystal structure of HIV-1 Vif ligase complex, where G71 is located within a solvent-exposed loop on the same surface as the α-helical D14-R15-M16-R17 motif previously implicated in interacting with A3F (Russell and Pathak, 2007; Russell et al., 2009; Smith and Pathak, 2010; Figure 3A). It is also consistent with huA3F E324 being located within the conserved α4 helix and likewise accessible for direct interaction (Figure 3B). In addition, E324 is part of the larger α3-α4 region of huA3F and rhA3F implicated by genetic studies as interacting with HIV-1 Vif (Albin et al., 2010b; Kitamura et al., 2012; Land et al., 2014; Russell and Pathak, 2007; Russell et al., 2009; Smith and Pathak, 2010).

We therefore used HIV-1 Vif G71 and huA3F E324 as anchoring points to generate a structural interaction model that obeys physical constraints and best explains prior genetic studies. The ClusPro protein-protein docking web server was used to generate 20 Vif-huA3F interaction models, and one model with Vif G71 and A3F E324 in close proximity was selected for further computational studies (Figure 3C). In this model the main chain amide of Vif G71 is within bonding distance of the side chain of A3F E324 (~3 Å). Additional features of this model are extensive interactions between the G71 loop and the DRMR motif of HIV-1 Vif with the α3 and α4 helices of A3F. In particular, Vif R15 is predicted to form a direct electrostatic interaction with A3F E289 (Figure 3C).

To optimize the predicted Vif-huA3F interface, the docked complex was subjected to three independent 1-μs MD simulations (Figures 3D, S2, and S3; Movies S1, S2, and S3). The first notable observation was the relative fragility of the interaction between Vif G71 and huA3F E324, which was lost rapidly in two of the simulations (persistence times of 70 and 1 ns in Movies S1 and S2; inter-residue distances plotted in Figure S2). Second, the electrostatic interaction between Vif R15 and huA3F E289 was stable through large proportions of each independent 1-μs simulation (Movies S1, S2, and S3; inter-residue distances plotted in Figure S3; representative pose in Figure 3D). Moreover, all three MD simulations arrived at a single preferred interaction conformation anchored by an interaction between Vif R15 and huA3F E289.

An additional appealing feature of these MD refinements was an approximately 90° rotation in the Vif interaction to include a hydrophobic pocket of huA3F between the α2 and α3 helices (Figure 3D; Movie S2). Specifically, Vif W79, which is located in the G71 loop, docked into the α2 and α3 hydrophobic pocket

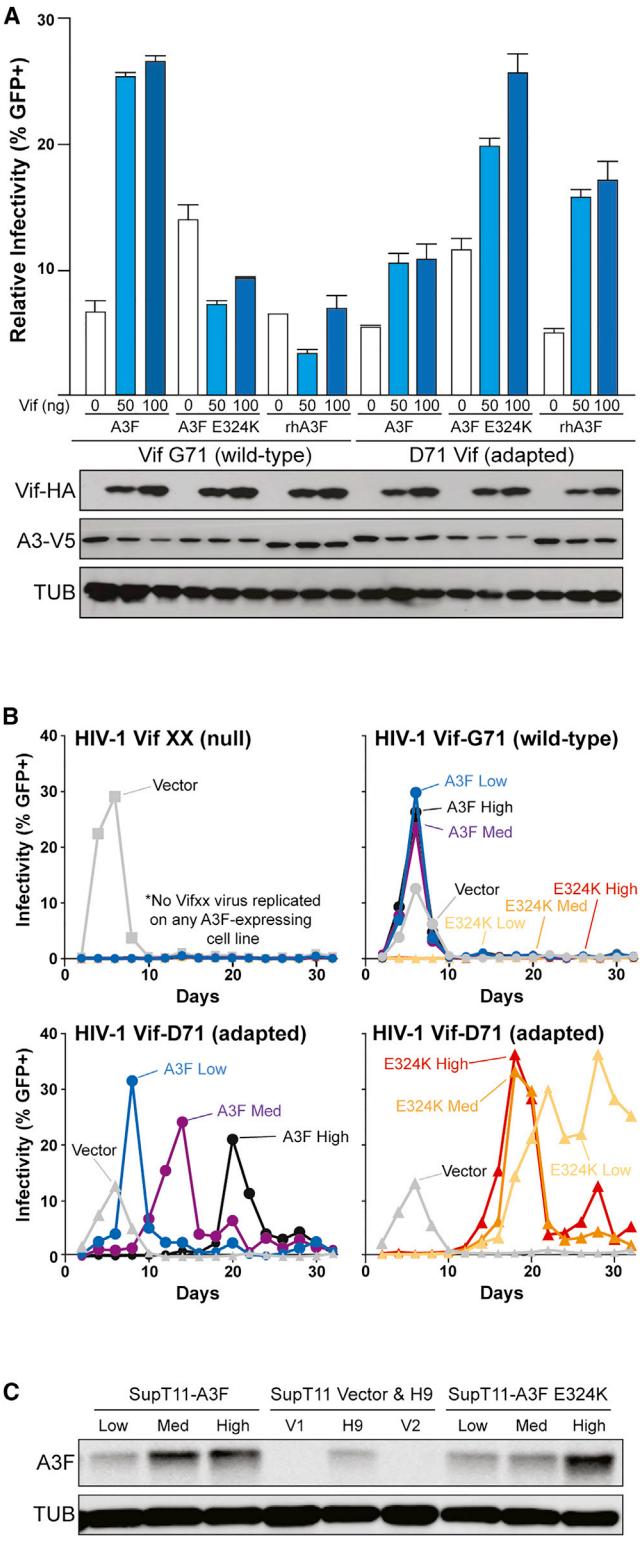

Figure 2. HIV-1 Vif G71D Enables Viral Infectivity in the Presence of Vif-Resistant A3F

(A) Single-cycle infectivity data for Vif-null HIV-1_{IIIB} produced in the presence of huA3F, huA3F E324K, or rhA3F and the indicated amounts of Vif G71 (wild-type) or Vif D71 (adapted) expression constructs. Immunoblots are shown below for Vif (anti-HA), A3F (anti-V5), and tubulin (anti-TUB).

(B) Spreading infection data are shown for HIV-1_{IIIB} stocks with the indicated Vif alleles in SupT11 clones expressing zero (empty vector), low, medium, or high levels of huA3F or huA3F E324K.

(C) Anti-A3F immunoblot of SupT11-derived T cell lines stably expressing huA3F or A3F E324K. Empty vector-transfected SupT11 clones V1 and V2 and the non-permissive T cell line H9 are shown for comparison.

of huA3F. This predicted interaction is concordant with prior mutagenesis experiments, which had implicated this huA3F region in the Vif interaction (Kitamura et al., 2012). In addition, this MD-optimized pose still maintains interactions between Vif and the α3 and α4 regions of huA3F, including the electrostatic interaction between Vif R15 and huA3F E289. Altogether, the MD simulation-optimized Vif interaction model buries approximately 1,300 $Å^2$ surface area between the two proteins and involves huA3F helices α2, α3, and α4, as well as the hydrophobic pocket between α2 and α3 (Figure 3D; Movie S2).

Model Validation

MD simulations predicted a direct electrostatic interaction between Vif R15 and A3F E289 (Figures 3D, S2, and S3; Movies S1, S2, and S3). Prior work showed that Vif R15A generated a separation-of-function variant defective for huA3F degradation, but not for A3G degradation, and also that huA3F E289K became resistant to HIV-1 Vif-mediated degradation (Russell and Pathak, 2007; Russell et al., 2009; Smith and Pathak, 2010). Thus, we predicted that reciprocal charge changes at these amino acid positions in Vif and huA3F, respectively, would singly destroy Vif degradation activity but together restore the functional interaction. Indeed, each of these charge-changing amino acid substitutions alone compromised Vif degradation function, but in combination the capacity for HIV-1 Vif to degrade huA3F was restored (Figure 4A). This result is evident through the decreased huA3F band intensities in immunoblot images (indicating degradation) and through significantly increased viral infectivity in single-cycle infection experiments. Additionally, this predicted gain-of-function pairing enabled HIV-1 with Vif E15 to undergo a robust spreading infection in SupT11 cells stably expressing the restrictive A3F K289 enzyme (Figure 4B). Taken together, these data provide strong genetic evidence in support of a direct physical interaction between Vif R15 and A3F E289 and the Vif-huA3F interaction model derived above.

DISCUSSION

The Vif-A3F interaction is essential for HIV-1 pathogenesis in humanized mice, rhesus macaques, and most likely also humans (Desrosiers et al., 1998; Farrow et al., 2005; Krisko et al., 2013; Rangel et al., 2009; Sato et al., 2014; Schmitt et al., 2010; Simon et al., 2005). Here we used huA3F E324K and rhesus A3F (naturally K324), which both resist degradation by HIV-1 Vif (Albin et al., 2010b; Hultquist et al., 2011; Virgen and Hatziioannou, 2007; Zennou and Bieniasz, 2006), as tools to select for viral variants that regain the capacity to replicate in long-term cell culture experiments. Vif G71D was the major adaptive change that emerged in these studies and the only one that reconfirmed

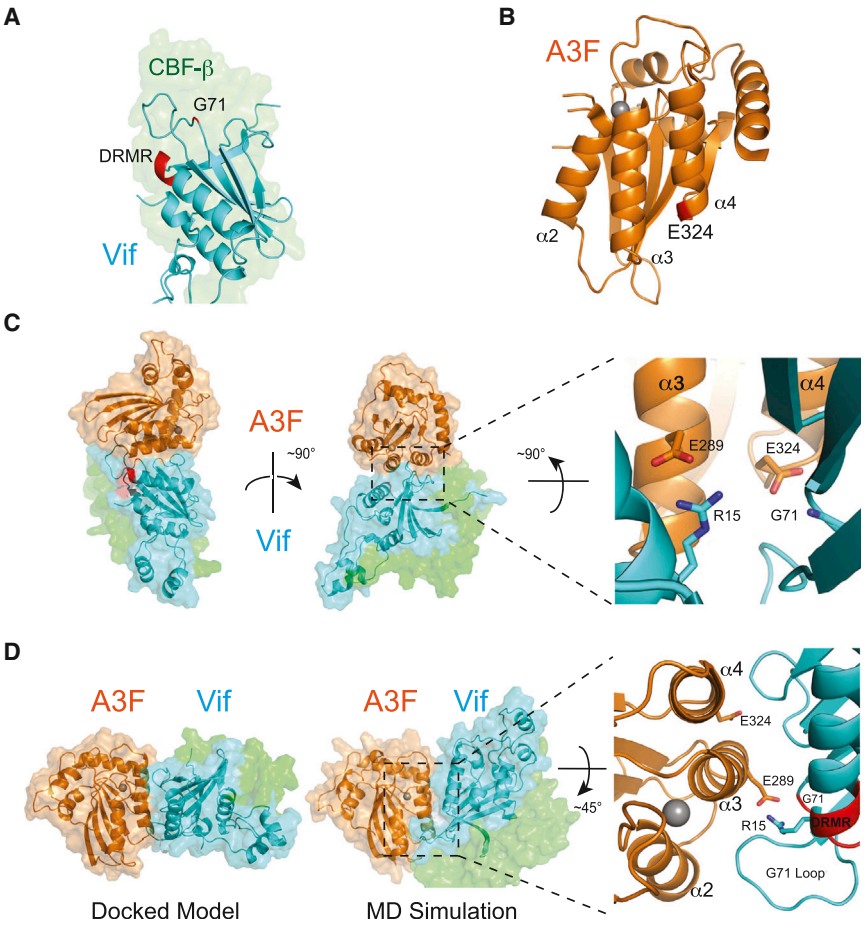

Figure 3. Vif-A3F Interaction Model

(A) A ribbon schematic of HIV-1 Vif highlighting residues D14, R15, M16, R17, and G71. D14 is the first residue of an α helix containing Vif residues 14–31, which includes the DRMR motif. Vif G71 is located in a nearby loop on the same surface of the structure (PDB: 4N9F). Vif is colored cyan and a faded surface representation of CBF-β is shown in green to facilitate visualization.

(B) A ribbon schematic shows the Vif-binding domain of huA3F, highlighting the α3 and α4 helices and the position of residue E324 near the end of the α4 helix (PDB: 4IOU).

(C) A model of the complex generated by docking A3Fctd onto Vif. In this initial docked model, direct interactions occur between A3F E324 and Vif G71 as well as A3F E289 and R15.

(D) An MD simulation-optimized model of the A3F-Vif macromolecular complex. Residues E289 and R15 form a strong persistent interaction, and residues within the Vif G71-containing loop are interacting with A3F residues between helices α2 and α3. See the main text for details.

in infectivity experiments. This infectivity-restoring amino acid change suggested that a new, stabilizing physical interaction had been established between A3F K324 and Vif D71, and it provided a critical constraint for docking studies. However, structural optimization using MD simulations suggested that the interaction between A3F E324 and Vif G71 is unlikely to be robust in the wild-type setting, and instead revealed a considerably more stable protein-protein interface dominated by a persistent electrostatic interaction between A3F E289 and Vif R15. Remarkably, the reciprocal charge changes of A3F E289K and Vif R15E resulted in A3F degradation and HIV-1 infectivity phenotypes similar to a wild-type scenario. These gain-of-function results provide strong genetic evidence in favor of A3F E289 and Vif R15 constituting an integral part of the physical interaction. The best-fit model presented here provides a comprehensive structural view of the A3F-Vif interaction and, by homology modeling, also of the entire A3F-bound ubiquitin ligase complex (Figure S5).

Prior mutagenesis studies have implicated multiple amino acids in the interaction between huA3F and HIV-1 Vif (Albin et al., 2010b; Kitamura et al., 2012; Land et al., 2014; Russell and Pathak, 2007; Russell et al., 2009; Smith and Pathak, 2010). Most of these prior results can be re-interpreted using our best-fit model and grouped into those that participate directly or indirectly in the actual interaction. Prior separation-of-function data include A3F amino acid substitutions C259K, IL262/3AA, S264D, and Y269A, which are located between the α2 and α3 helices, and E289K and E324K, which are located on the solvent-exposed surfaces of the α3 and α4 helices, respectively. Each of these A3F amino acid substitutions confer resistance to Vif-mediated degradation and do not affect the enzyme's HIV-1 restriction capabilities (Albin et al., 2010b; Kitamura et al., 2012; Land et al., 2014; Russell and Pathak, 2007; Russell et al., 2009; Smith and Pathak, 2010; this study). These A3F residues are all located within the interface of our best-fit model, best highlighted by A3F E289 forming a persistent electrostatic interaction with Vif R15.

On the Vif side of this interaction, separation-of-function mutants fall into three clusters. Vif cluster 1 residues are located in an α helix defined by D14, R15, M16, and R17 (Russell and Pathak, 2007; Russell et al., 2009; Schröfelbauer et al., 2006; Smith and Pathak, 2010). Our model indicates that this HIV-1 Vif helix forms extensive electrostatic interactions with A3F α3 and α4 helices (e.g., Vif R15 with A3F E289). Vif cluster 2 residues span the G71 loop region (residues G71–G82) (Figures 3C and S4). Our model predicts that this aligns Vif W79 to dock with residues located between the α2 and α3 helices of A3F. Several single alanine substitutions within this loop confer susceptibility to A3F-mediated restriction (e.g., E76A in Figure S4). Vif cluster 3 residues (H42, H43, and Y44) are predicted to interact with amino acids located between A3F α3 and α4 helices. Although this region of Vif clearly mediates interactions with A3G (Kouno et al., 2015; Russell and Pathak, 2007; Russell et al., 2009; Smith and Pathak, 2010), our model suggests that these residues also may participate in the Vif-A3F interaction. Overall, Vif clusters 1, 2, and 3 may combine

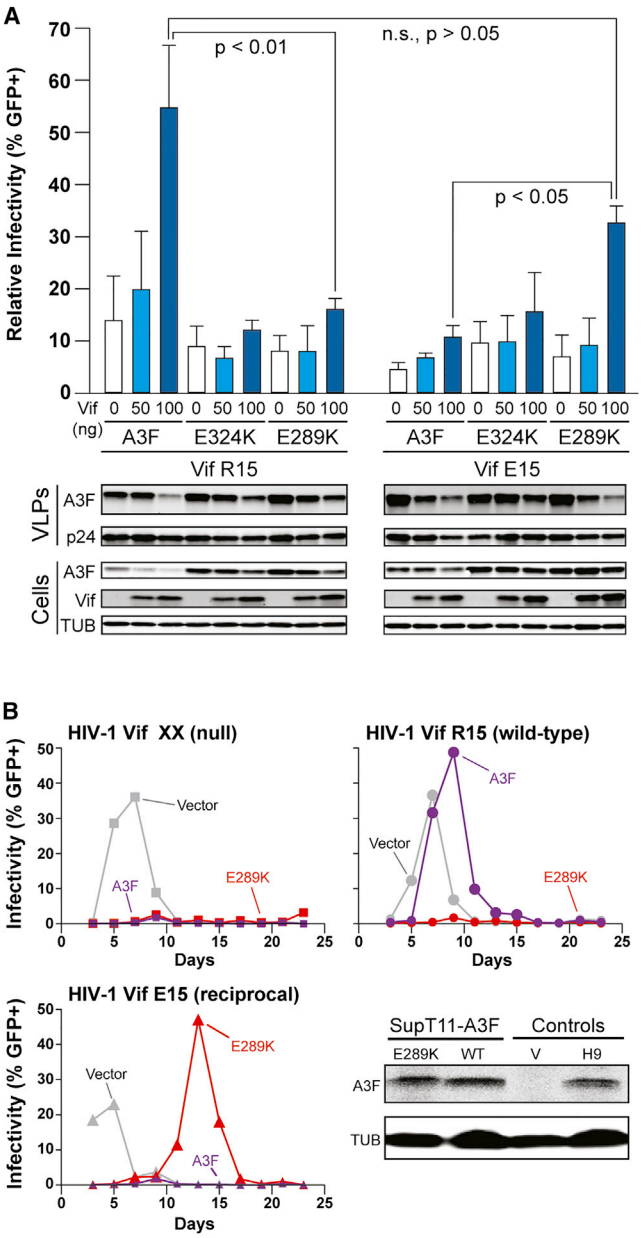

Figure 4. HIV-1 Vif-A3F Interface Interactions Validated by Gain-of-Function Viral Infectivity Experiments

(A) Single-cycle infectivity data for Vif-null HIV-1_{IIIB} produced in the presence of huA3F, huA3F E324K, or huA3F E289K and the indicated amounts of Vif R15 (wild-type) or Vif E15 expression constructs. Each histogram bar shows the average infectivity from three independent experiments (mean ± SEM). Statistical significance was determined by two-way ANOVA followed by a post hoc Bonferroni test to determine significance between or within testing groups (p values of less than 0.05 were considered significant). Immunoblots are shown below for virus-like particles (anti-A3F and anti-P24) and producer cell lysates (anti-A3F, anti-Vif, and anti-TUB).

(B) Spreading infection data demonstrate that HIV-1 encoding Vif R15E replicates on SupT11 that stably expresses A3F E289K, whereas HIV-1 IIIB Vif cannot establish a productive infection in identical culture conditions. SupT11-derived T cell lines used for these spreading infections have been stably transfected with huA3F, A3F E289K, or a vector. A3F protein expression in H9 lysates is shown for comparison.

to bind A3F, with clusters 1 and 2 forming essential interactions and cluster 3 providing additional stabilizing contacts.

We propose a wobble model to explain the dynamic nature of the Vif-A3 interaction (Figure 5). In this model, Vif forms a network of interactions with a given A3 substrate, such as A3F. If the overall interaction is destabilized, for instance, due to an immune escape variation in Vif or a naturally occurring variation in a host A3 enzyme, a compensatory change in Vif can restore a fully functional interaction. Such a compensatory change may occur at the original interacting residue, nearby, or even at an edge of the interface. In support of this idea, the negatively charged mutation G71D was selected in multiple independent adaptation experiments in order to counteract a positively charged E324K substitution in huA3F or the naturally occurring K324 in rhesus macaque A3F, yet this interaction was weak in MD simulations. On an evolutionary timescale, an extensive series of wobbles could enable the Vif-A3 interface to drift to a completely different solvent-exposed surface (Figure 5). This model provides an attractive explanation for how HIV-1 Vif could have evolved to use distinct surfaces to bind each of the restrictive human A3 enzymes (e.g., A3F and A3G in Figure 5; data in this study; Albin et al., 2010b; Kitamura et al., 2012; Kouno et al., 2015; Land et al., 2014; Ooms et al., 2013; Refsland et al., 2014; Russell and Pathak, 2007; Russell et al., 2009; Smith and Pathak, 2010). It also provides a molecular explanation for the evolutionary theory known as the Red Queen's Hypothesis (Van Valen, 1973). Moreover, based on the relatively facile cross-species adaptation of HIV-1 from huA3F- to rhesus macaque A3F-expressing cells, this model accounts for how an ancestral lentivirus may have adapted from a host with a simple A3 repertoire (most non-primate mammals) to be able to replicate in the presence of a more complex, multi-protein A3 repertoire, as exists in modern primates including humans (Figure 5). This wobble model also may explain the evolutionary dynamics of a wide range of pathogen-host interactions.

EXPERIMENTAL PROCEDURES

Plasmids

The huA3F-matching NM_145298 and A3F QE323-324EK have been described previously (Albin et al., 2010b; Liddament et al., 2004). Rhesus A3F-matching NM_001042373.1 was provided by T. Hatziioannou (Aaron Diamond AIDS Research Center [ADARC]) and cloned into a pcDNA3.1-derived 3× hemagglutinin (HA) vector as described previously (Liddament et al., 2004). A V5-tagged derivative of rhA3F was made by subcloning from the 3×HA vector as described previously (Albin et al., 2010b). Specific point mutants were made by QuikChange site-directed mutagenesis (Stratagene). Full-length proviral HIV_{IIIB} and $HIV_{LAI-GFP}$ plasmids have been described, and the HIV_{IIIB} sequence is identical to EU541617 except for an A200C nucleotide change to interrupt an atypical upstream open reading frame (Albin et al., 2010b; Haché et al., 2008, 2009). Proviral mutant plasmid mutants were assembled in a TOPO shuttle vector containing the *vif-vpr* region and then subcloned back into the full-length context via the unique sites SwaI/SalI in HIV-1_{IIIB} or PshAI/SalI in HIV-$1_{LAI-GFP}$.

Cell Culture

T cell lines were maintained in RPMI supplemented with 10% fetal bovine serum, penicillin/streptomycin, and β-mercaptoethanol. The 293T cells were maintained in DMEM supplemented with 10% fetal bovine serum and penicillin/streptomycin. Stable APOBEC3-expressing cell lines have been described and new lines were established using the same methods (Albin et al., 2010a, 2010b; Hultquist et al., 2011).

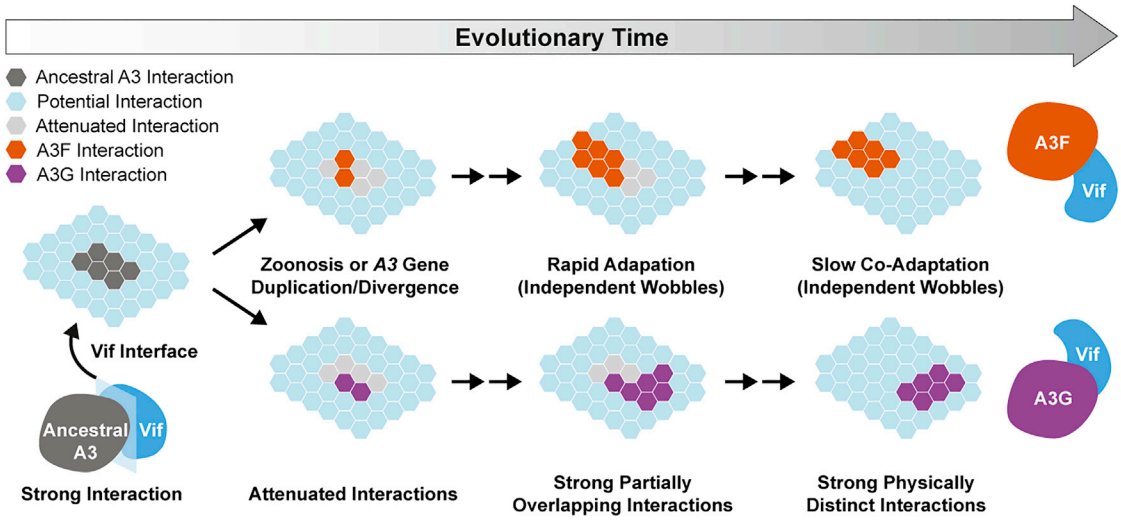

Figure 5. Wobble Model to Explain the Evolution of the Vif-A3 Interaction

The schematic shows the wobble model for adaptation of the Vif side of the Vif-A3 interface. Each hexagon of the lattice depicts a potential interaction as follows: ancestral, dark gray; potential, light blue; attenuated, light gray; A3F, orange; and A3G, purple. The model predicts that the ancestral Vif-A3 interaction was strong and consisted of six interaction points (arbitrary number for discussion purposes). Viral transmission to a new host with a larger A3 repertoire results in diminished but still partly functional interactions. A series of rapid adaptations (possibly most or all in the original new host) restores the strong interaction and results in partly overlapping interaction surfaces. Then, over a much longer evolutionary period, the combined effect of many independent wobbles triggered by virus or host genetic changes could result in the present day non-overlapping surfaces of Vif that interact with A3F and A3G. Similar rules would apply to other HIV-1-restrictive A3s (not shown for simplicity). A strong interaction may be disrupted by a viral or host amino acid substitution mutation, but the overall interaction can be restored by a compensatory change in Vif at the same site, nearby, or even to extend the edge of an interaction surface. If this change occurs at a new position, it can be considered a wobble. A series of wobbles over evolutionary time can account for a shift in the entire interaction surface.

HIV-1 Adaptation and Infectivity Studies

The selection protocol was carried out as described in the text and depicted in Figure 1A. Adapted viruses were selected for molecular characterization if fourth-passage infectivity exceeded 2% absolute CEM-GFP infectivity for viruses adapted to A3F QE323-324EK or at least 5% for viruses adapted to rhA3F. Adapted *vif* genotypes were identified by preparing genomic DNA from infected CEM-GFP reporter cells (PureGene), amplifying the *vif-vpr* region as described previously (Albin et al., 2010a), and sequencing each PCR product (Genewiz). Chromatograms were inspected manually to identify mutations. Spreading infections were performed as described previously (Albin et al., 2010a). Single-cycle infectivity studies were done as described using an HIV-1_{IIIB} Vif-deficient proviral plasmid, APOBEC3F-V5 or an A3F-untagged construct, and codon-optimized HIV-1_{IIIB} Vif-HA constructs (Albin et al., 2010a, 2010b; Hultquist et al., 2011).

Immunoblotting

Primary antibodies were mouse (Ms) anti-V5 (Invitrogen), rabbit (Rb) anti-A3F (NIH AIDS Reagent Program 11474 courtesy of M. Malim), Ms anti-HA.11 (Covance), Ms anti-HIV-1 p24/CA (AIDS Reagent Program 3537 courtesy of B. Chesebro and K. Wehrly), Ms anti-HIV-1 Vif (AIDS Reagent Program 6459 courtesy of M. Malim), and Ms anti-tubulin (Covance). Secondary antibodies were donkey anti-Ms IgG-HRP (Jackson Laboratory) and goat anti-Rb IgG-HRP (Bio-Rad). Additional secondary antibodies were IRdye 800CW goat anti-Rb (LI-COR Biosciences 827-08365) and Alexa Fluor 680 goat anti-Ms (Molecular Probes A-21057). Membranes were imaged using commercial chemiluminescence reagents (Denville Scientific) and film or a LI-COR Odyssey instrument. A subset of the LI-COR images were prepared for presentation using Image J 1.49 (http://rsb.info.nih.gov/ij/download.html).

Statistical Analysis

GraphPad Prism 5.0 was used for statistical analyses (GraphPad). Quantitative data are presented as mean ± SEM. Statistical significance was determined by two-way ANOVA followed by a post hoc Bonferroni test to determine significance between or within testing groups. A p value of less than 0.05 was considered statistically significant.

SUPPLEMENTAL INFORMATION

Supplemental Information includes Supplemental Experimental Procedures, five figures, three movies, and two data files and can be found with this article online at http://dx.doi.org/10.1016/j.celrep.2015.10.067.

AUTHOR CONTRIBUTIONS

C.R., J.S. Albin, and R.S.H. designed the virology experiments. C.R., J.S. Albin, E.M.L., A.M.L., J.R.H., and J.S. Anderson performed virology experiments. C.R., J.S. Albin, E.M.L., A.M.L., B.D.A., D.A.H., and R.S.H. analyzed data from virology experiments. R.E.A., O.D., and N.M.S. designed and implemented the computational experiments. N.M.S. created the structural model of the A3F-Vif ligase complex. R.S.H. conceived and B.D.A. illustrated the wobble model for rapid evolution of pathogen-host interactions. R.S.H. drafted the manuscript and C.R., O.D., N.M.S., and B.D.A. drafted the figures. All authors edited and approved the final manuscript.

ACKNOWLEDGMENTS

We thank the AIDS Research and Reference Reagent Program for materials. This research was supported by the National Institute of Allergy and Infectious Diseases (NIAID) R01 AI064046 and the National Institute of General Medical Sciences (NIGMS) P01 GM091743 to R.S.H. Partial salary support was provided by NIGMS T32 GM008244 (University of Minnesota Medical Scientist Training Program) and National Institute on Drug Abuse (NIDA) F30 DA026310 to J.S. Albin, NIAID T32 AI83196 (IMV Training Program) to C.R., and NIH T32 AI007313 (Immunology Training Program) and NIAID F31

AI116305 to B.D.A. The computational components were funded in part by the NIH Director's New Innovator Award Program DP2-OD007237, National Biomedical Computation Resource NIH P41 GM103426, and National Science Foundation (NSF) XSEDE Supercomputer resources grant RAC CHE060073N to R.E.A. R.S.H. is an Investigator of the Howard Hughes Medical Institute.

Received: June 27, 2015
Revised: September 10, 2015
Accepted: October 22, 2015
Published: November 25, 2015

REFERENCES

Albin, J.S., Haché, G., Hultquist, J.F., Brown, W.L., and Harris, R.S. (2010a). Long-term restriction by APOBEC3F selects human immunodeficiency virus type 1 variants with restored Vif function. J. Virol. *84*, 10209–10219.

Albin, J.S., LaRue, R.S., Weaver, J.A., Brown, W.L., Shindo, K., Harjes, E., Matsuo, H., and Harris, R.S. (2010b). A single amino acid in human APOBEC3F alters susceptibility to HIV-1 Vif. J. Biol. Chem. *285*, 40785–40792.

Anderson, B.D., and Harris, R.S. (2015). Transcriptional regulation of APOBEC3 antiviral immunity through the CBF-β/RUNX axis. Sci. Adv. *1*, e1500296.

Bishop, K.N., Holmes, R.K., Sheehy, A.M., Davidson, N.O., Cho, S.J., and Malim, M.H. (2004). Cytidine deamination of retroviral DNA by diverse APOBEC proteins. Curr. Biol. *14*, 1392–1396.

Bohn, M.F., Shandilya, S.M., Albin, J.S., Kouno, T., Anderson, B.D., McDougle, R.M., Carpenter, M.A., Rathore, A., Evans, L., Davis, A.N., et al. (2013). Crystal structure of the DNA cytosine deaminase APOBEC3F: the catalytically active and HIV-1 Vif-binding domain. Structure *21*, 1042–1050.

Desimmie, B.A., Delviks-Frankenberrry, K.A., Burdick, R.C., Qi, D., Izumi, T., and Pathak, V.K. (2014). Multiple APOBEC3 restriction factors for HIV-1 and one Vif to rule them all. J. Mol. Biol. *426*, 1220–1245.

Desrosiers, R.C., Lifson, J.D., Gibbs, J.S., Czajak, S.C., Howe, A.Y., Arthur, L.O., and Johnson, R.P. (1998). Identification of highly attenuated mutants of simian immunodeficiency virus. J. Virol. *72*, 1431–1437.

Farrow, M.A., Somasundaran, M., Zhang, C., Gabuzda, D., Sullivan, J.L., and Greenough, T.C. (2005). Nuclear localization of HIV type 1 Vif isolated from a long-term asymptomatic individual and potential role in virus attenuation. AIDS Res. Hum. Retroviruses *21*, 565–574.

Guo, Y., Dong, L., Qiu, X., Wang, Y., Zhang, B., Liu, H., Yu, Y., Zang, Y., Yang, M., and Huang, Z. (2014). Structural basis for hijacking CBF-β and CUL5 E3 ligase complex by HIV-1 Vif. Nature *505*, 229–233.

Haché, G., Liddament, M.T., and Harris, R.S. (2005). The retroviral hypermutation specificity of APOBEC3F and APOBEC3G is governed by the C-terminal DNA cytosine deaminase domain. J. Biol. Chem. *280*, 10920–10924.

Haché, G., Shindo, K., Albin, J.S., and Harris, R.S. (2008). Evolution of HIV-1 isolates that use a novel Vif-independent mechanism to resist restriction by human APOBEC3G. Curr. Biol. *18*, 819–824.

Haché, G., Abbink, T.E., Berkhout, B., and Harris, R.S. (2009). Optimal translation initiation enables Vif-deficient human immunodeficiency virus type 1 to escape restriction by APOBEC3G. J. Virol. *83*, 5956–5960.

Harris, R.S., and Dudley, J.P. (2015). APOBECs and virus restriction. Virology *479-480*, 131–145.

Hultquist, J.F., Lengyel, J.A., Refsland, E.W., LaRue, R.S., Lackey, L., Brown, W.L., and Harris, R.S. (2011). Human and rhesus APOBEC3D, APOBEC3F, APOBEC3G, and APOBEC3H demonstrate a conserved capacity to restrict Vif-deficient HIV-1. J. Virol. *85*, 11220–11234.

Kitamura, S., Ode, H., Nakashima, M., Imahashi, M., Naganawa, Y., Kurosawa, T., Yokomaku, Y., Yamane, T., Watanabe, N., Suzuki, A., et al. (2012). The APOBEC3C crystal structure and the interface for HIV-1 Vif binding. Nat. Struct. Mol. Biol. *19*, 1005–1010.

Kouno, T., Luengas, E.M., Shigematsu, M., Shandilya, S.M., Zhang, J., Chen, L., Hara, M., Schiffer, C.A., Harris, R.S., and Matsuo, H. (2015). Structure of the Vif-binding domain of the antiviral enzyme APOBEC3G. Nat. Struct. Mol. Biol. *22*, 485–491.

Krisko, J.F., Martinez-Torres, F., Foster, J.L., and Garcia, J.V. (2013). HIV restriction by APOBEC3 in humanized mice. PLoS Pathog. *9*, e1003242.

Land, A.M., Shaban, N.M., Evans, L., Hultquist, J.F., Albin, J.S., and Harris, R.S. (2014). APOBEC3F determinants of HIV-1 Vif sensitivity. J. Virol. *88*, 12923–12927.

Liddament, M.T., Brown, W.L., Schumacher, A.J., and Harris, R.S. (2004). APOBEC3F properties and hypermutation preferences indicate activity against HIV-1 *in vivo*. Curr. Biol. *14*, 1385–1391.

Ooms, M., Brayton, B., Letko, M., Maio, S.M., Pilcher, C.D., Hecht, F.M., Barbour, J.D., and Simon, V. (2013). HIV-1 Vif adaptation to human APOBEC3H haplotypes. Cell Host Microbe *14*, 411–421.

Rangel, H.R., Garzaro, D., Rodríguez, A.K., Ramírez, A.H., Ameli, G., Del Rosario Gutiérrez, C., and Pujol, F.H. (2009). Deletion, insertion and stop codon mutations in vif genes of HIV-1 infecting slow progressor patients. J. Infect. Dev. Ctries. *3*, 531–538.

Refsland, E.W., Hultquist, J.F., and Harris, R.S. (2012). Endogenous origins of HIV-1 G-to-A hypermutation and restriction in the nonpermissive T cell line CEM2n. PLoS Pathog. *8*, e1002800.

Refsland, E.W., Hultquist, J.F., Luengas, E.M., Ikeda, T., Shaban, N.M., Law, E.K., Brown, W.L., Reilly, C., Emerman, M., and Harris, R.S. (2014). Natural polymorphisms in human APOBEC3H and HIV-1 Vif combine in primary T lymphocytes to affect viral G-to-A mutation levels and infectivity. PLoS Genet. *10*, e1004761.

Russell, R.A., and Pathak, V.K. (2007). Identification of two distinct human immunodeficiency virus type 1 Vif determinants critical for interactions with human APOBEC3G and APOBEC3F. J. Virol. *81*, 8201–8210.

Russell, R.A., Smith, J., Barr, R., Bhattacharyya, D., and Pathak, V.K. (2009). Distinct domains within APOBEC3G and APOBEC3F interact with separate regions of human immunodeficiency virus type 1 Vif. J. Virol. *83*, 1992–2003.

Sato, K., Takeuchi, J.S., Misawa, N., Izumi, T., Kobayashi, T., Kimura, Y., Iwami, S., Takaori-Kondo, A., Hu, W.S., Aihara, K., et al. (2014). APOBEC3D and APOBEC3F potently promote HIV-1 diversification and evolution in humanized mouse model. PLoS Pathog. *10*, e1004453.

Schmitt, K., Hill, M.S., Liu, Z., Ruiz, A., Culley, N., Pinson, D.M., and Stephens, E.B. (2010). Comparison of the replication and persistence of simian-human immunodeficiency viruses expressing Vif proteins with mutation of the SLQYLA or HCCH domains in macaques. Virology *404*, 187–203.

Schröfelbauer, B., Senger, T., Manning, G., and Landau, N.R. (2006). Mutational alteration of human immunodeficiency virus type 1 Vif allows for functional interaction with nonhuman primate APOBEC3G. J. Virol. *80*, 5984–5991.

Simon, V., Zennou, V., Murray, D., Huang, Y., Ho, D.D., and Bieniasz, P.D. (2005). Natural variation in Vif: differential impact on APOBEC3G/3F and a potential role in HIV-1 diversification. PLoS Pathog. *1*, e6.

Siu, K.K., Sultana, A., Azimi, F.C., and Lee, J.E. (2013). Structural determinants of HIV-1 Vif susceptibility and DNA binding in APOBEC3F. Nat. Commun. *4*, 2593.

Smith, J.L., and Pathak, V.K. (2010). Identification of specific determinants of human APOBEC3F, APOBEC3C, and APOBEC3DE and African green monkey APOBEC3F that interact with HIV-1 Vif. J. Virol. *84*, 12599–12608.

Van Valen, L. (1973). A new evolutionary law. Evol. Theory *1*, 1–30.

Virgen, C.A., and Hatziioannou, T. (2007). Antiretroviral activity and Vif sensitivity of rhesus macaque APOBEC3 proteins. J. Virol. *81*, 13932–13937.

Wiegand, H.L., Doehle, B.P., Bogerd, H.P., and Cullen, B.R. (2004). A second human antiretroviral factor, APOBEC3F, is suppressed by the HIV-1 and HIV-2 Vif proteins. EMBO J. *23*, 2451–2458.

Zennou, V., and Bieniasz, P.D. (2006). Comparative analysis of the antiretroviral activity of APOBEC3G and APOBEC3F from primates. Virology *349*, 31–40.

Zheng, Y.H., Irwin, D., Kurosu, T., Tokunaga, K., Sata, T., and Peterlin, B.M. (2004). Human APOBEC3F is another host factor that blocks human immunodeficiency virus type 1 replication. J. Virol. *78*, 6073–6076.